Contact Angle of Surfactant Solutions on Precipitated Surfactant Surfaces. II. Effects of Surfactant Structure, Presence of a Subsaturated Surfactant, pH, and Counterion/Surfactant Ratio

Piyada Balasuwatthi[a], Nimit Dechabumphen[a], Chintana Saiwan[a], and John F. Scamehorn[b],*

[a]Petroleum and Petrochemical College, Chulalongkorn University, Bangkok 10330, Thailand, and [b]Institute for Applied Surfactant Research, University of Oklahoma, Norman, Oklahoma 73019

ABSTRACT: The contact angle of a saturated aqueous surfactant solution on the precipitate of that surfactant was measured by using the sessile drop method. The sodium and calcium salts of alkyl sulfates (C_{12}, C_{14}, and C_{18}) had advancing contact angles higher than those of alkyl trimethylammonium bromides (C_{14}, C_{16}, and C_{18}). The measured advancing contact angles for several surfactant solutions did not substantially change with varying surfactant/counterion ratios; therefore, the precipitating counterion concentration (e.g., water hardness) had little effect on the wettability. The contact angles of fatty acid (C_{12} and C_{16}) solutions did not show any dependence on pH between a pH of 4 and 10. The contact angles of saturated calcium dodecanoate (CaC_{12}) solutions containing a second subsaturated surfactant (sodium dodecyl sulfate: NaDS) decreased with increasing NaDS concentrations until reaching the critical micelle concentration of the surfactant mixture. These results show that the second surfactant can act as a wetting agent in this saturated surfactant system. Application of Young's equation to contact angles showed that the solid/liquid surface tension can change substantially with surfactant concentration and be important in addition to the liquid/vapor surface tension in reducing contact angles. Application of the Zisman equation results in a "critical" surface tension for the CaC_{12} or soap scum of 25.5 mN/m, which is comparable to difluoroethene.
Paper no. S1329 in *JSD 7*, 31–40 (January 2004).

KEY WORDS: Contact angle, defoamer, hydrophobicity, wetting.

Wettability of solid surfaces by surfactants is an important property that is manipulated in numerous practical applica-

*To whom correspondence should be addressed at 100 East Boyd, School of Chemical Engineering and Materials Science, University of Oklahoma, Norman, OK 73019. E-mail: scamehor@ou.edu

Abbreviations: γ_{LV}, liquid/vapor interfacial tension; γ_{SL}, solid/liquid interfacial tension; γ_{SV}, solid/vapor interfacial tension; θ or θ_A, advancing contact angle; $C_{14}TAB$, tetradecyl trimethylammonium bromide; $C_{16}TAB$, hexadecyl trimethylammonium bromide; $C_{18}TAB$, octadecyl trimethylammonium bromide; CaC_{12}, calcium dodecanoate; CaDS, calcium dodecyl sulfate; CMC, critical micelle concentration; K_{SP}, solubility product constant; NaDS, sodium dodecyl sulfate.

tions such as oil recovery, printing, coating, adhesion, flotation, and detergency and that is also used as an analytical technique to characterize surfaces in basic material research (1). Surfactants are often used to enhance the wetting ability of an aqueous solution since they can modify the solid/liquid and liquid/vapor interfacial tension (2–4). The ability of a liquid to spread over a solid surface is controlled by the overall free energy at the interfaces. If spreading of a liquid results in lowering the total free energy at the interfaces, then the wetting process can occur spontaneously (5). Adsorption of anionic or cationic surfactants on nonpolar solids such as Teflon can change the interfacial tension and contact angle (6–9). Adsorption of surfactant onto surfactant crystals during the precipitation process can affect both the kinetics of surfactant precipitation (10) and the surfactant's crystal habit (11,12). One practical application of the present work was to test the proposed dewetting mechanism (hydrophobic nature of the particles of a calcium/magnesium precipitate with the soap destabilizing foam lamellae) used to explain the antifoam behavior of soap in hard water (13).

Wetting, in its most general sense, is the displacement from a surface of one fluid by another. In the case of an aqueous solution spreading over a solid, as studied here, the tendency for fluids to wet can be indicated by the contact angle. A low contact angle (near 0°) means high wettability, and a high contact angle (>90°) means poor wettability.

The relationship between the interfacial tensions of the surfaces at the three-phase boundary of a solid/liquid/vapor system at equilibrium is described by the Young equation (14):

$$\gamma_{SV} - \gamma_{SL} = \gamma_{LV} \cos \theta \qquad [1]$$

where γ_{SV}, γ_{SL}, and γ_{LV} are solid/vapor, solid/liquid, and liquid/vapor interfacial tensions, respectively, and θ is the equilibrium contact angle. This is only valid for a liquid drop resting at equilibrium on a smooth, flat, homogeneous, impermeable, and nondeformable surface, but it is used as a model for explaining wetting phenomena in most other systems.

The measurement of contact angle is the most rapid and convenient way of characterizing the simultaneous interaction between solid, liquid, and vapor phases. If a liquid with well-known properties is used for the measurement, the resulting interfacial tension can be used to identify the nature of the solid used (15); for example, the contact angle of water has commonly been used as a criterion for evaluating the hydrophobicity of a surface (16,17).

Many experimental techniques are available for contact angle measurement, such as capillary penetration techniques (14,18), the adhering gas bubble method (19), the Wilhelmy plate method, and the sessile drop technique (20,21). In the sessile drop method used in this study, contact angles are measured directly by depositing a drop of liquid on a solid surface and placing a tangent to the drop at its base manually or by a computer program. The resulting "static advancing contact angle" represents the "equilibrium contact angle." Some operator subjectivity can affect the measurement, and the positions of the tangent line and the baseline of the droplet are estimated by sight. The images are often small, making precision extremely difficult. In addition, the optical phenomenon known as parallax can cause inconsistency between measurements (15). Moreover, obtaining a valid, reproducible contact angle is more difficult than it appears for a number of reasons: contamination of the droplet, surface cleanliness, surface heterogeneity, surface roughness, and environmental conditions (21). These factors resulted in a precision of about ±5° in the measurement of contact angle in this work. Since the variables studied here generally have a substantial effect on contact angle, this precision is adequate for our purposes.

In part I of this series (22), the contact angle of surfactant solutions on precipitated surfactant surfaces was discussed for the first time. In that work, the contact angles of saturated solutions of sodium and calcium salts of both fatty acids and alkyl sulfates of varying alkyl chain lengths and of free fatty acids of varying alkyl chain lengths were measured on a solid precipitated surfactant of the same type (only one surfactant present in the system). In this work, contact angles for cationic surfactants, fatty acids at different pH levels, and anionic surfactants at different counterion/surfactant ratios in solution were studied for single surfactant systems. Also reported here are contact angles on precipitated surfactant surfaces where the solution contained the precipitated surfactant at saturation and a second subsaturated surfactant. The change in interfacial tension at the air/water and solid/water interfaces attributable to this subsaturated surfactant is related to contact angle and surfactant adsorption.

EXPERIMENTAL PROCEDURES

Materials. The cationic surfactants, tetradecyl trimethylammonium bromide (C_{14}TAB, 98% purity), hexadecyl trimethylammonium bromide (C_{16}TAB, 98% purity), and octadecyl trimethylammonium bromide (C_{18}TAB, 97% purity) were obtained from Fluka (Steinheim, Germany) and used without further purification. Sodium dodecyl sulfate (NaDS, >99% purity), from Sigma Chemical Co. (St. Louis, MO), and sodium tetradecyl sulfate (95% purity) and sodium octadecyl sulfate (93% purity), from Aldrich Chemical Co. (Milwaukee, WI), were used without further purification. The fatty acids used in this study were dodecanoic acid (>99% purity; Sigma) and hexadecanoic acid (95% purity; Sigma). Calcium salts of fatty acids were prepared by adding 20% excess calcium chloride to the surfactant solutions. The precipitate obtained from the reaction was filtered and rinsed with distilled water and dried in an oven at 40°C for 24 h. Sodium bromide (99.5% purity) and calcium chloride dihydrate (UNIVAR grade) were obtained from Ajax Chemical Co (Auburn, Australia). Doubly distilled and deionized water with a maximum conductivity of 2 µmho/cm was used for the preparation of solutions throughout these experiments.

Sample preparation. (i) Saturated solution preparation. All surfactant solutions were prepared at saturated conditions for contact angle measurement. The saturated solutions of cationic surfactants were prepared by dissolving the surfactant in doubly distilled and deionized water until no more dissolution occurred. In the case of C_{14}TAB and C_{16}TAB, the solutions were saturated by adding sodium bromide in different quantities to satisfy the solubility product. In the case of NaDS, sodium chloride was used instead of sodium bromide. Since the solutions can remain supersaturated for a long time, all the solutions were cooled to 0°C to force precipitation and placed in a controlled water bath at 30°C, shaken periodically, and allowed to equilibrate for at least 4 d.

(ii) Surfactant mixture preparation. The surfactant solution of 100 mM NaDS in a saturated calcium dodecanoate (CaC_{12}) solution was prepared as a stock solution. The solution was then diluted with a saturated CaC_{12} solution to obtain surfactant mixtures with various NaDS concentrations.

(iii) Solid sample preparation. Solid samples of precipitated surfactant were made by using a hydraulic press (Biorad P/N 15011) with a highly polished stainless steel punch and die of 13 mm diameter. The sample was compressed at 10-ton force with a 3-min dwelling time to obtain a smooth and reflective surface. Samples with nonuniform surfaces were rejected. The pellets were stored in a controlled humidity desiccator at ambient temperature prior to use.

Methods. (i) pH adjustment. The effect of pH on contact angles of saturated solutions of dodecanoic or hexadecanoic acid was studied by adjusting the pH with hydrochloric acid and sodium hydroxide and measuring the pH with a pH meter (Benchtop pH/ISE Meter, Model 420A, with triode pH electrode Model 91-578N).

(ii) Solubility product. The saturated solution of surfactant ions in equilibrium with its precipitates was filtered using a 0.22-µm cellulose acetate membrane, and the filtrate solution was analyzed for the equilibrium concentration of surfactant. The concentrations of surfactant solutions were measured using a total organic carbon analyzer (TOC-5000A; Shimadzu). The bromide concentrations were measured by an ion chromatograph (Hewlett-Packard Series1050) with

an Alltech Anion/R column (10 µm, 150 × 4.6 mm; Alltech, Deerfield, IL) and conductivity detector (Alltech 350). The sample solution was loaded into a 100-µL sample loop and injected into the column using pure methanol as a mobile phase at the flow rate of 1 mL/min. Sodium and calcium concentrations were measured by using an atomic absorption spectrophotometer (Varian Spectra AA300). Absorption measurement of calcium was made in a nitrous oxide–acetylene flame at 422.7 nm wavelength, and sodium was measured in an air–acetylene flame at 589 nm wavelength.

(iii) Contact angle measurement. The contact angles were measured by using the sessile drop technique. The apparatus consisted of a camera with a micro lens and a closed plexiglas chamber with the dimensions of 21 × 27 × 15 cm. There was a rectangular gate of 10 × 15 cm at the front panel for insertion of the sample and a hole of 0.5 cm at the top of the chamber for microsyringe injection for adding or withdrawing solution onto the droplet. The chamber was connected to the thermostat to control temperature. Before measurement, the chamber environment was preheated at 30 ± 1°C by switching on the thermostat and was saturated with water vapor to prevent a drop evaporation effect. When the temperature reached 30°C, the precipitated surface was placed in a closed plexiglas chamber. The solution drop was introduced onto the surface through a microsyringe and made to advance or retreat by adding or withdrawing a small volume of solution (20–70 µL). The advancing or receding contact angles were measured by taking photographic images after adding or withdrawing the solution for 15 s. The contact angles were determined directly from the photographs by drawing tangent lines between the liquid drop and the solid surface using a computer with a Photoshop program as illustrated in Figure 1. The measurement was made on both sides of the drop and the average was taken. In this paper, only advancing contact angles are reported (as θ or θ_A); receding contact angles are discussed in part I of this series (22).

(iv) Surface tension measurement (ASTM D1331-89) (23). The surface tension of the surfactant solution was determined by using a DuNoüy-ring technique (KRÜSS digital tensiometer, Model K10ST) with a platinum–iridium ring that had a wetting length of 199.95 mm, a ring radius of 9.6545 mm, and a wire radius of 0.185 mm. All surface tension measurements were controlled at 30 ± 0.5°C. The ring was rinsed with water and heated in the gas flame of an alcohol burner before use to remove impurities. The precision of the surface tension of water was ±0.3%. The vessel was rinsed with the solution sample before use. The solution was added to the vessel and the ring was then dipped into the solution. The instrument was then switched on and the surface tension measured when equilibrium was attained. Each surface tension was the average of at least 10 readings. All necessary precautions were taken to maximize accuracy (24). The critical micelle concentrations (CMC) were determined from a break point in plots of surface tension as a function of bulk surfactant concentration.

(v) Adsorption measurement. The adsorption of subsaturated NaDS onto the surfactant precipitate was determined by measuring the concentration of NaDS before and after adsorption (solution depletion method). The NaDS in saturated solutions of CaC_{12} (20 mL) was added to a vial containing 0.5 g of CaC_{12} precipitate and allowed to equilibrate at 30°C for 4 d in a water bath. The samples were then centrifuged by a high-speed centrifuge (Sorval Super T21) at 3000 rpm for 10 min, filtered, and the supernatant solutions analyzed for equilibrium NaDS concentration.

(vi) Analysis. The concentration of NaDS was analyzed by high-performance liquid chromatography (Hewlett-Packard series 1050) with a conductivity detector (Alltech Model 550) and a C_{18} reversed-phase silica column (Alltech Alltima, 5 µm × 150 mm × 4.6 mm). The temperature of the detector was adjusted to 30°C. The carrier solvent was composed of 60% methanol and 40% water at a flow rate of 0.5 mL/min. Each sample solution was analyzed in duplicate.

RESULTS

Solubility product. The precipitated surfactant can be in equilibrium with different ratios of surfactant and counterion (calcium, sodium, or hydrogen) below the CMC as long as the solubility product is satisfied. If distilled water is equilibrated with a pure ionic surfactant crystal, the surfactant ion and the counterion (e.g., cation for the anionic surfactant) will be present in solution in their stoichiometric proportions. This surfactant/counterion ratio could be different if, for example, hard water were equilibrated with an anionic surfactant crystal. In this study, activity coefficients were ignored in calculating and using apparent or concentration-based K_{SP} values; therefore, in the range of high salt concentrations, the apparent K_{SP} values for the solutions were not comparable to activity-based values from the literature. For our purposes, as long as activity coefficients did not vary much with surfactant concentration (a good approximation at the relatively low surfactant concentrations and ionic strengths used here), the concentration-based K_{SP} values did not vary with changing counterion concentrations. For divalent counterion calcium, the K_{SP} was defined as
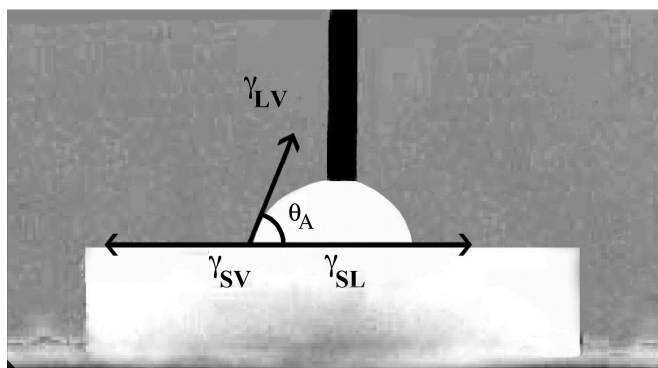
FIG. 1. Sessile-drop contact angle method. θ_A is the advancing contact angle; γ_{SV}, γ_{SL}, and γ_{LV} are solid/vapor, solid/liquid, and liquid/vapor interfacial tensions, respectively.

$$K_{SP} = \left[Ca^{2+}\right]\left[S^-\right]^2 \qquad [2]$$

and for monovalent sodium,

$$K_{SP} = \left[Na^+\right]\left[S^-\right] \qquad [3]$$

for the solution in equilibrium with the precipitate, where $[S^-]$ is the surfactant anion concentration. These apparent concentration-based K_{SP} values are shown in Table 1.

Effect of surfactant structure and counterion type. The values of the advancing contact angles (θ_A) as a function of the number of carbons in the hydrophobe (n) for sodium alkyl sulfate, calcium alkyl sulfate, and alkyl trimethylammonium bromide are shown in Table 2. The contact angles of sodium and calcium salts of alkyl sulfates (C_{12}, C_{14}, and C_{18}) were in the range of 46 to 96° and increased when the alkyl chain length increased, particularly when the alkyl chain length was above 14 (22). The alkyl trimethylammonium bromides (C_{14}, C_{16}, and C_{18}) had contact angles between 0 and 34°, with the contact angle increasing with increasing alkyl chain length. The contact angle for C_{18}TAB was not highly accurate since there was penetration from the solution into the precipitated surface, which reduced the contact angle. Therefore, the contact angles of this surfactant shown in Table 2 are approximate values and are provided to show the trend with varying alkyl chain lengths for this series of cationic surfactants. Figure 2 shows plots of advancing contact angles vs. carbon chain length of the surfactant hydrophobe for these cationic surfactants, as well as the calcium and sodium salts of alkyl sulfates for comparison.

Nonstoichiometric ratio of surfactant to counterion. From Equations 2 and 3, the solubility product can be satisfied at different ratios of counterion/surfactant ion for a given counterion and surfactant. Table 3 shows advancing contact angles for sodium and calcium salts of alkyl sulfates, CaC_8, and CaC_{12}. The surfactant concentration was set by addition of the surfactant with a counterion, which was not present in the precipitate (solubility product not met), and the equilibrium concentration of the precipitating counterion was measured. The same K_{SP} for a given surfactant anion/counterion pair (Table 3) was not observed at different surfactant concentrations owing to imprecisions in counterion concentration measurements, but the expected

TABLE 1
Solubility Product Constant (K_{SP}) Values for Sodium and Calcium Salts of Alkyl Sulfates, Calcium Octanoate, and Calcium Dodecanoate at 30°C

Surfactant	K_{SP} (concentration-based)
NaDS (sodium dodecyl sulfate)	2.63×10^{-4} M^2
CaDS (calcium dodecyl sulfate)	2.65×10^{-11} M^3
NaTS (sodium tetradecyl sulfate)	2.59×10^{-6} M^2
CaTS (calcium tetradecyl sulfate)	6.30×10^{-12} M^3
NaOS (sodium octadecyl sulfate)	7.82×10^{-8} M^2
CaOS (calcium octadecyl sulfate)	1.09×10^{-13} M^3
CaC$_8$ (calcium octanoate)	4.53×10^{-7} M^3
CaC$_{12}$ (calcium dodecanoate)	1.43×10^{-12} M^3

TABLE 2
Advancing Contact Angles (θ_A) of Single-Component Saturated Surfactant Solutions on Precipitated Surfactants at 20–70 μL Drop Volumes[a]

Surfactant	Average θ_A (degree)
NaDS	56
NaTS	56
NaOS	72
CaDS	46
CaTS	47
CaOS	96
C$_{14}$TAB (tetradecyl trimethylammonium bromide)	0–2
C$_{16}$TAB (hexadecyl trimethylammonium bromide)	16
C$_{18}$TAB (octadecyl trimethylammonium bromide)	34

[a]For other abbreviations see Table 1.

trend was seen. The results show that θ_A had little systematic dependence on the surfactant/counterion ratio for all systems. However, for the most water-soluble surfactant studied (NaDS), the contact angle was less reproducible (more data scatter) than the less soluble surfactants. These results indicate that the precipitating counterion concentration (e.g., water hardness) will have little effect on wettability for saturated single-component surfactant systems.

Effect of pH of fatty acid solutions. The contact angles for saturated fatty acid solutions (C_{12}, C_{16}) with pH ranging from 4.0 to 10.0 onto its own precipitate surface are shown in Figure 3. Dodecanoic acid had a contact angle of 77 to 81°, whereas the contact angle of hexadecanoic acid varied from 82 to 84° over this pH range.

Effect of subsaturated surfactant. (i) Liquid/vapor surface tension and CMC values. The CMC of the surfactant solution containing saturated CaC_{12} and subsaturated NaDS concentrations was determined by plotting the liquid/vapor surface tension (γ_{LV}) as a semilogarithmic function of NaDS concentration as shown in Figure 4. The break point in the slope is the CMC. The CMC values were taken at 7.8 mM for the pure NaDS solution and at 6.5 mM for the mixture of saturated CaC_{12} and NaDS at 30°C. The CMC value obtained for the pure NaDS solution at 30°C agrees with literature values (25,26). The CMC of CaC_{12} could not be measured because the solubility of CaC_{12} was too low at 30°C.

(ii) Contact angle. The advancing contact angles of a saturated CaC_{12} solution containing subsaturated NaDS are
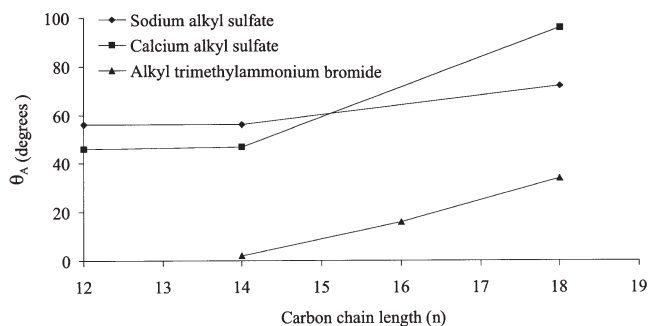
FIG. 2. θ_A of sodium alkyl sulfate, calcium alkyl sulfate, and alkyl trimethylammonium bromide. For abbreviation see Figure 1.

TABLE 3
θ_A **for Nonstoichiometric Saturated Solutions of Single-Component Surfactants**

Surfactant	Average θ_A (degree)
NaDS	
$[DS^-] = 1.44 \times 10^{-4}$ M, $[Na^+] = 4.057$ M	67
$[DS^-] = 1.54 \times 10^{-4}$ M, $[Na^+] = 1.509$ M	54
$[DS^-] = 1.72 \times 10^{-4}$ M, $[Na^+] = 1.326$ M	54
$[DS^-] = 1.85 \times 10^{-4}$ M, $[Na^+] = 2.543$ M	56
$[DS^-] = 2.10 \times 10^{-4}$ M, $[Na^+] = 1.252$ M	50
$[DS^-] = 2.39 \times 10^{-4}$ M, $[Na^+] = 2.839$ M	58
CaDS	
$[DS^-] = 1.94 \times 10^{-4}$ M, $[Ca^{2+}] = 9.23 \times 10^{-4}$ M	45
$[DS^-] = 2.11 \times 10^{-4}$ M, $[Ca^{2+}] = 4.49 \times 10^{-4}$ M	49
$[DS^-] = 3.64 \times 10^{-4}$ M, $[Ca^{2+}] = 2.00 \times 10^{-4}$ M	46
$[DS^-] = 4.72 \times 10^{-4}$ M, $[Ca^{2+}] = 8.38 \times 10^{-4}$ M	43
$[DS^-] = 5.60 \times 10^{-4}$ M, $[Ca^{2+}] = 7.06 \times 10^{-4}$ M	47
$[DS^-] = 1.01 \times 10^{-3}$ M, $[Ca^{2+}] = 8.73 \times 10^{-4}$ M	48
NaTS	
$[TS^-] = 6.51 \times 10^{-4}$ M, $[Na^+] = 5.65 \times 10^{-3}$ M	58
$[TS^-] = 6.66 \times 10^{-4}$ M, $[Na^+] = 7.83 \times 10^{-3}$ M	56
$[TS^-] = 8.54 \times 10^{-4}$ M, $[Na^+] = 2.17 \times 10^{-3}$ M	54
$[TS^-] = 8.65 \times 10^{-4}$ M, $[Na^+] = 1.48 \times 10^{-3}$ M	54
$[TS^-] = 1.06 \times 10^{-3}$ M, $[Na^+] = 1.13 \times 10^{-3}$ M	67
$[TS^-] = 1.10 \times 10^{-3}$ M, $[Na^+] = 2.09 \times 10^{-3}$ M	50
CaTS	
$[TS^-] = 9.58 \times 10^{-5}$ M, $[Ca^{2+}] = 7.88 \times 10^{-4}$ M	44
$[TS^-] = 1.02 \times 10^{-4}$ M, $[Ca^{2+}] = 3.29 \times 10^{-4}$ M	48
$[TS^-] = 1.08 \times 10^{-4}$ M, $[Ca^{2+}] = 2.99 \times 10^{-4}$ M	53
$[TS^-] = 1.10 \times 10^{-4}$ M, $[Ca^{2+}] = 1.22 \times 10^{-3}$ M	45
$[TS^-] = 1.12 \times 10^{-4}$ M, $[Ca^{2+}] = 6.11 \times 10^{-4}$ M	44
$[TS^-] = 1.26 \times 10^{-4}$ M, $[Ca^{2+}] = 6.09 \times 10^{-4}$ M	51
NaOS	
$[OS^-] = 5.04 \times 10^{-5}$ M, $[Na^+] = 1.96 \times 10^{-3}$ M	95
$[OS^-] = 5.16 \times 10^{-5}$ M, $[Na^+] = 3.50 \times 10^{-3}$ M	96
$[OS^-] = 5.99 \times 10^{-5}$ M, $[Na^+] = 6.26 \times 10^{-4}$ M	94
$[OS^-] = 6.97 \times 10^{-5}$ M, $[Na^+] = 5.74 \times 10^{-4}$ M	94
$[OS^-] = 7.54 \times 10^{-5}$ M, $[Na^+] = 1.17 \times 10^{-3}$ M	95
$[OS^-] = 9.36 \times 10^{-5}$ M, $[Na^+] = 2.61 \times 10^{-4}$ M	99
CaOS	
$[OS^-] = 1.87 \times 10^{-5}$ M, $[Ca^{2+}] = 3.54 \times 10^{-4}$ M	72
$[OS^-] = 2.00 \times 10^{-5}$ M, $[Ca^{2+}] = 3.46 \times 10^{-4}$ M	69
$[OS^-] = 2.42 \times 10^{-5}$ M, $[Ca^{2+}] = 9.98 \times 10^{-5}$ M	74
$[OS^-] = 2.87 \times 10^{-5}$ M, $[Ca^{2+}] = 1.70 \times 10^{-4}$ M	72
$[OS^-] = 2.93 \times 10^{-5}$ M, $[Ca^{2+}] = 8.86 \times 10^{-5}$ M	71
$[OS^-] = 3.16 \times 10^{-5}$ M, $[Ca^{2+}] = 1.17 \times 10^{-4}$ M	75
CaC$_8$	
$[C_8^-] = 0.0068$ M, $[Ca^{2+}] = 2.74 \times 10^{-3}$ M	93
$[C_8^-] = 0.0091$ M, $[Ca^{2+}] = 4.64 \times 10^{-3}$ M	92
$[C_8^-] = 0.0103$ M, $[Ca^{2+}] = 5.31 \times 10^{-3}$ M	94
$[C_8^-] = 0.0132$ M, $[Ca^{2+}] = 4.86 \times 10^{-3}$ M	92
CaC$_{12}$	
$[C_{12}^-] = 4.49 \times 10^{-5}$ M, $[Ca^{2+}] = 5.74 \times 10^{-4}$ M	85
$[C_{12}^-] = 4.79 \times 10^{-5}$ M, $[Ca^{2+}] = 3.49 \times 10^{-4}$ M	83
$[C_{12}^-] = 5.81 \times 10^{-5}$ M, $[Ca^{2+}] = 3.24 \times 10^{-4}$ M	85
$[C_{12}^-] = 1.04 \times 10^{-4}$ M, $[Ca^{2+}] = 2.44 \times 10^{-4}$ M	82
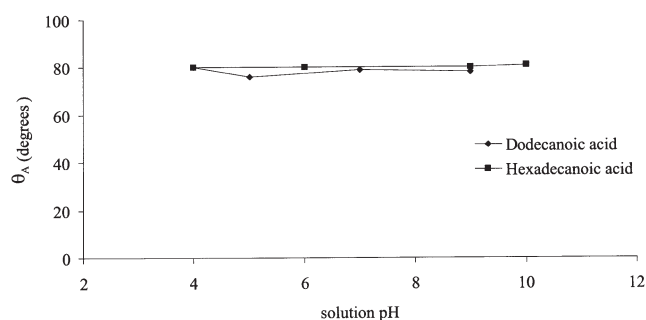
FIG. 3. θ_A of dodecanoic acid and hexadecanoic acid. For abbreviation see Figure 1.

shown in Figure 5. The contact angles decreased significantly with increasing NaDS concentration until reaching a plateau above the system CMC of 6.5 mM.

(iii) Adsorption of the subsaturated surfactant onto the precipitated surfactant. The adsorption isotherm of NaDS onto the CaC_{12} precipitate is shown in Figure 6. At a low concentration of surfactant, the increase in adsorption with surfactant concentration was a less-than-proportional increase (for a proportional relationship, the slope of adsorption vs. equilibrium concentration on a log–log plot is unity). At NaDS concentrations above the CMC, after a plateau region, the adsorption appeared to increase sharply. The amount of NaDS adsorbing in the neighborhood of the CMC was 70 μmol/g (20 μmol/m^2 or 8.3 Å^2/molecule).

(iv) Calculation of solid/liquid surface tension. From Equation 1, if γ_{SV} and γ_{SL} are constant, the plot of $\cos\theta$ vs. $1/\gamma_{LV}$ should be linear and slope = $(\gamma_{SV} - \gamma_{SL})$. The results in Figure 7 do not show this linear relationship, indicating that γ_{SL} varied with surfactant concentration. The value of γ_{SV} can reasonably be assumed to be independent of the surfactant concentration because the dry solid had not yet been contacted by the liquid in an advancing contact angle. Even if the NaDS adsorbed as a complete bilayer on the flat surface of the precipitated surfactant, the reduction in NaDS concentration due to adsorption-induced depletion would be a maximum of 22%. Therefore, the initial NaDS concentration was assumed to be the same as the equilibrium NaDS concentration, ignoring this small correction. There is no simple way to measure or calculate the absolute value of γ_{SL}. However, we can calculate γ_{SL} relative to γ_{SL} at a reference state (γ_{SL}^0). The reference state chosen was that corresponding to no NaDS being present. Subtracting Equation 1 for the condition of interest from Equation 1 for the standard state condition yields:

$$\gamma_{LV}^0 (\cos\theta)^0 - \gamma_{LV}(\cos\theta) = (\gamma_{SV} - \gamma_{SL})^0 - (\gamma_{SV} - \gamma_{SL})$$
$$= (\gamma_{SL} - \gamma_{SL}^0) \quad [4]$$

Rearrangement of Equation 4 yields

$$(\gamma_{LV}^0 / \gamma_{LV})(\cos\theta)^0 - \cos\theta = (\gamma_{SL}/\gamma_{LV}) - (\gamma_{SL}^0/\gamma_{LV}) \quad [5]$$

where the superscript ^{0} refers to the standard state when no NaDS is added to the solution, i.e., the CaC_{12} saturated
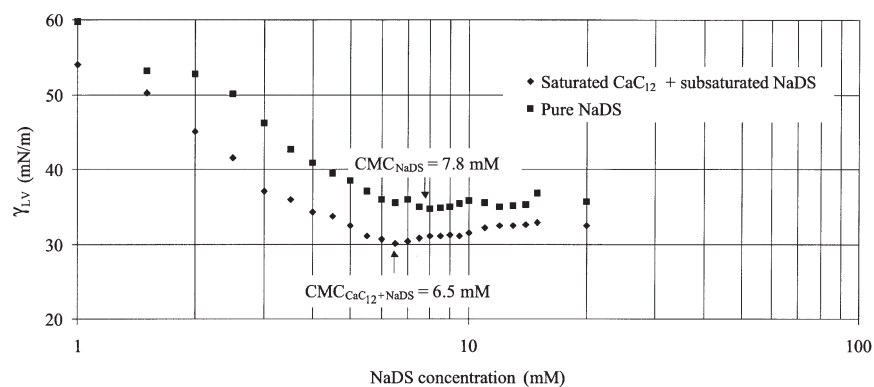
FIG. 4. γ_{LV} as a function of sodium dodecyl sulfate (NaDS) concentration. Pure NaDS and a mixed solution of saturated calcium dodecanoate (CaC$_{12}$) and subsaturated NaDS. CMC, critical micelle concentration. For other abbreviations see Figure 1.
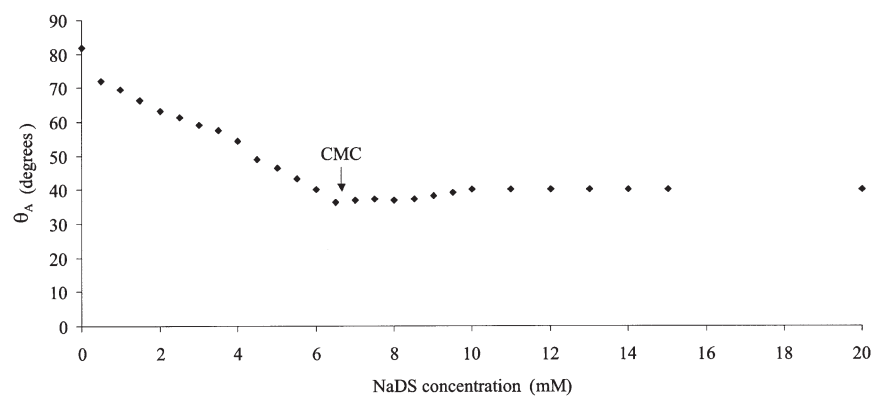
FIG. 5. θ_A of a saturated CaC$_{12}$ solution with varying NaDS concentrations. For abbreviations see Figures 1 and 4.
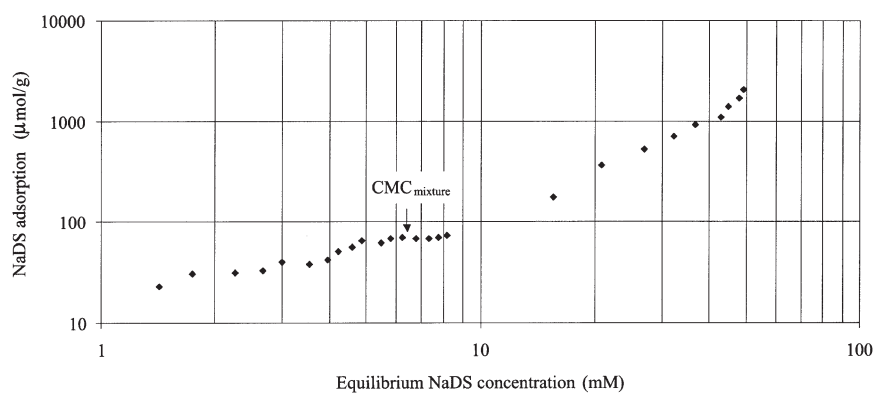
FIG. 6. Adsorption of NaDS onto a CaC$_{12}$ precipitate. For abbreviations see Figure 4.
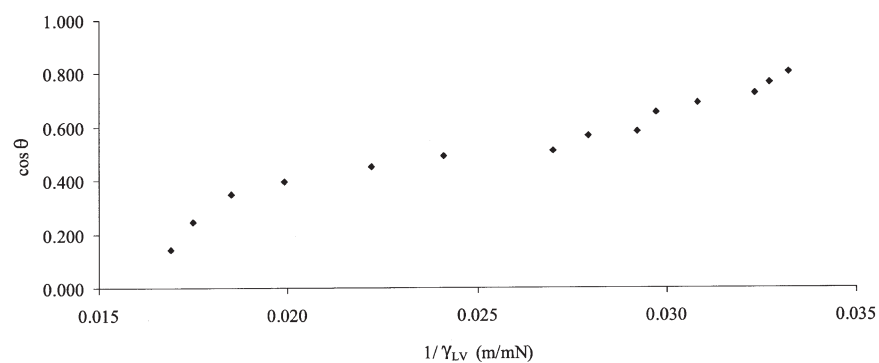
FIG. 7. Contact angle as related to γ_{LV} of a mixed solution of saturated CaC$_{12}$ and subsaturated NaDS. For abbreviations see Figures 1 and 4.

solution. The γ_{SL} is the solid/liquid surface tension of the mixed surfactant solution at a given NaDS concentration.

Using the adsorption data from Figure 6, the relative solid/liquid surface tension ($\gamma_{SL} - \gamma_{SL}^{0}$) could be correlated

to surfactant adsorption density on the solid as well as to surfactant concentration. The value of γ_{LV} could be obtained from the data in Figure 4. The reduction in solid/liquid surface tension ($\gamma_{SL}^{0} - \gamma_{SL}$) of saturated CaC$_{12}$ contain
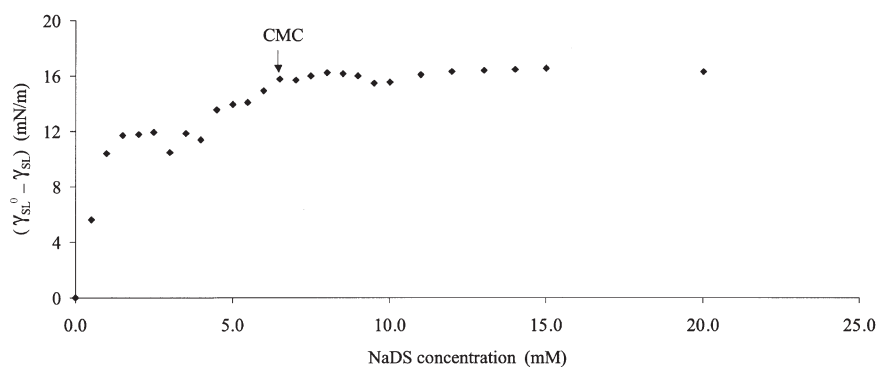
FIG. 8. Solid/liquid spreading pressure $(\gamma_{SL}^0 - \gamma_{SL})$ of a mixed solution of saturated CaC_{12} and subsaturated NaDS as a function of NaDS concentration. For abbreviations see Figures 1 and 4.
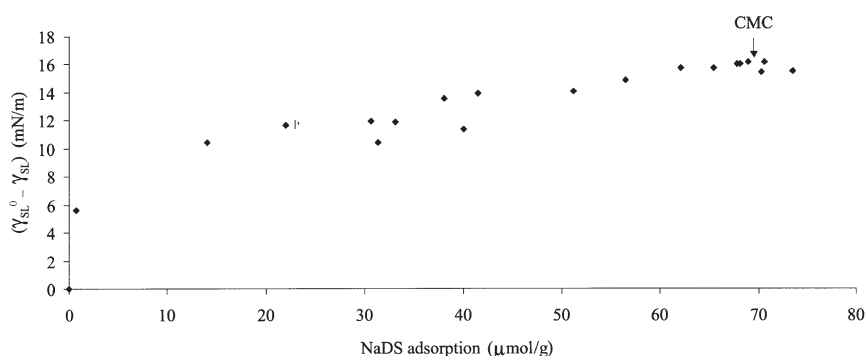
FIG. 9. $\gamma_{SL}^0 - \gamma_{SL}$ of a mixed solution of saturated CaC_{12} and subsaturated NaDS as a function of NaDS adsorption. For abbreviations see Figures 1, 4, and 8.

ing NaDS as a function of NaDS concentration and NaDS adsorption is shown in Figures 8 and 9, respectively. The parameter $(\gamma_{SL}^0 - \gamma_{SL})$ is a spreading pressure for the solid/liquid interface, representing the reduction in surface tension induced by the presence of the subsaturated surfactant. However, unlike liquid/vapor spreading pressures, the value of the surface tension for the "pure solvent" or standard state was not measurable.

DISCUSSION

Effect of surfactant structure and counterion type. The contact angles of the sodium and calcium salts of alkyl sulfates were high compared to those of alkyl trimethylammonium bromides with similar hydrophobic sizes, as shown in Figure 2. Cationic surfactants (e.g., quaternary ammonium headgroups) generally have a higher CMC than anionic surfactants (e.g., sulfate headgroups) (14) with the same hydrophobic group size. Even when the cationic and anionic surfactants were compared on the basis of similar CMC values ($C_{18}TAB$ was roughly equivalent to a sodium alkyl sulfate with 15 carbons based on the CMC), from Figure 2, the contact angle of the cationic surfactant was smaller than that of the alkyl sulfate. This may be related to the larger hydrophilic group of the trimethylammonium group compared to the sulfate group.

Effect of pH of fatty acid solutions. Figure 3 shows that the contact angles of both dodecanoic acid and hexadecanoic acid are almost independent of pH. According to Drelich *et al.* (27), the extent of dissociation of carboxylic groups depends on the pH of the aqueous phase, and significant

dissociation of carboxylic groups can be expected to occur in the solution under alkaline conditions. The pK_a of sodium octanoate is 5.3 (28) and should depend little on the hydrophobe chain length of the surfactant. Therefore, the range of pH values studied here (4–10) corresponds to almost completely protonated (neutral) surfactants to almost completely ionized anionic surfactants. Since the solid precipitate must be almost electrically neutral, there is one hydrogen (or hydronium) ion per surfactant anion in the crystalline solid. However, as pH varies, the ratio of ionized surfactant/neutral (protonated) surfactant in solution changes. Therefore, the fact that the value of θ_A had almost no dependence on pH for the fatty acid (Fig. 3) indicates that the protonated and unprotonated surfactants had approximately the same surface activity at the solid/liquid and liquid/vapor interfaces.

Effect of a subsaturated surfactant. Figure 5 shows that the subsaturated surfactant acted as an effective wetting agent on the precipitated CaC_{12}, with more than a 40° decrease in contact angle attributable to added NaDS, despite the fact that the solution was already saturated with CaC_{12}. In part I of this series (22), we showed that saturated solutions of sodium alkyl sulfates, calcium alkyl sulfates, sodium salts of fatty acids, calcium salts of fatty acids, and free fatty acids very rarely had a contact angle that exceeded 90° with the solid precipitate of that surfactant. This was interpreted as not supporting the concept that soaps act as defoamers/antifoams in hard water *via* the mechanism of dewetting of "hydrophobic" soap precipitates. This work provides even more evidence against the dewetting theory of foam regulation since in applications such as laundry detergency, where

soluble surfactants are present with the soap, it is an effective foam-control agent. As shown for the calcium soap used here, a contact angle of <40° in the presence of the subsaturated surfactant was observed, resulting in a fairly hydrophilic solid. Such a low contact angle implies that the NaDS was adsorbing in a headgroup-out configuration (e.g., a bilayer or a tail-down/head-out monolayer).

The adsorption isotherm in Figure 6 shows a slope of less than unity on a log–log plot, indicating a lack of cooperation between the adsorbed surfactant molecules. This indicates that adsorption increased gradually without a two-dimensional phase change to form admicelles, as is often observed on highly hydrophilic surfaces such as metal oxides (29). The adsorption density of NaDS in the vicinity of CMC was used to calculate the area per adsorbed surfactant molecule of 8.3 Å^2. The area occupied per molecule for DS$^-$ in the compact monolayer reported by Dahanayake *et al.* (30) was 53 Å^2. The calculated result indicated that there were approximately six layers of DS$^-$ adsorbing on the solid surface. Unless surfactant precipitation was occurring simultaneously, more than two adsorbing layers are not generally thought to occur in surfactant adsorption (31). Below the CMC, the NaDS did not exceed its K_{SP} with either sodium or calcium ($K_{SP_{NaDS}} = 2.63 \times 10^{-4}$ M^2; $K_{SP_{CaDS}} = 2.65 \times 10^{-11}$M^3). We suspected that the surface of the CaC$_{12}$ precipitate was modified during the drying process at 40°C in an oven and possibly changed the surface area of the precipitate because the CaC$_{12}$ precipitate had a low melting point (48°C). As a result, the surface area of precipitated CaC$_{12}$ was reduced and the area/adsorbed molecule calculation was inaccurate. As seen in Figure 6, after plateauing at the CMC, surfactant adsorption increased dramatically. As micelles were formed above the mixed-system CMC, these mixed micelles were composed of both the dodecyl sulfate and dodecanoate anionic surfactants. As NaDS concentration increased above the CMC, a higher concentration of micelles was formed, causing some precipitated CaC$_{12}$ to dissolve to allow the dodecanoate to micellize. Although a stoichiometric ratio of calcium/surfactant dissolved, less than a stoichiometric amount of counterions bound onto micelles (32), so some of the dissolved calcium ended up unassociated in solution. When this calcium concentration became high enough, the calcium/dodecyl sulfate K_{SP} was exceeded and precipitation of the DS$^-$ occurred as the calcium salt. As more NaDS was added, more CaC$_{12}$ dissolved and more calcium dodecyl sulfate (CaDS) precipitated. Since the solution depletion method of measuring adsorption used here was unable to differentiate adsorption from precipitation, the "apparent" adsorption reported in Figure 6 increased with NaDS concentration above the CMC. This combination of adsorption and precipitation was defined as "abstraction" by Hanna and Somasundaran (33) and was observed by Smith *et al.* (34). Therefore, in Figure 9 where the relative solid/liquid interfacial tension is plotted against surfactant adsorption, the concentration range where CaDS precipitation is occurring was not included since we wished to correlate surface parameters to true adsorption. As shown in Figure 7, the contact

angle decreased as γ_{LV} decreased due to an increasing NaDS concentration below the CMC. Both γ_{LV} (Fig. 5) and θ_A (Fig. 4) became nearly constant above the CMC. Normally, surfactant adsorption on a solid changes little above the CMC (31); the increase observed here (Fig. 6) is believed to be due to NaDS precipitation. Therefore, further discussion will focus on the sub-CMC region.

Wetting enhancement by surfactants is commonly attributed primarily to a reduction in liquid/vapor surface tension. For example, the well-known Zisman equation (35) attributes contact angle changes of pure fluids on low-energy surfaces solely to liquid/vapor surface tension. From Equation 1, this implies that γ_{SL} is constant or, from Equation 5, that the ratio (γ_{SL}/γ_{LV}) is constant. Even though the Zisman equation was originally confined to pure liquids, it is now widely used (or misused) for surfactant solutions. As seen in Figure 8, γ_{SL} decreased by approximately 16 mN/m between no added NaDS and the CMC, whereas γ_{LV} decreased by about 30 mN/m (for no added NaDS, $\gamma_{LV} = 59$ mN/m) over this same range, all with saturated CaC$_{12}$. Increasing adsorption of the NaDS onto the CaC$_{12}$ precipitate was the cause of the decrease in γ_{SL} as the NaDS concentration increased, just as NaDS adsorption at the vapor/liquid interface was responsible for the reduction in γ_{LV} as the NaDS concentration increased. Figure 9 shows the dependence of the solid/liquid spreading pressure on surfactant adsorption at this interface.

The Zisman equation is as follows (20,35):

$$\cos \theta = 1 - \beta\left(\gamma_{LV} - \gamma_{LV}{}^c\right) \qquad [6]$$

where $\gamma_{LV}{}^c$ is the critical surface tension characteristic of the solid. A Zisman plot is a graph of cos θ vs. γ_{LV} from which $\gamma_{LV}{}^c$ and β are deduced. The value of $\gamma_{LV}{}^c$ represents the maximum surface tension of a liquid that results in a contact angle of 0° and results in wetting. Values of $\gamma_{LV}{}^c$ have been tabulated for many hydrophobic polymers (20). Figure 10 shows the Zisman plot for the CaC$_{12}$/NaDS system studied here. The Zisman equation is not obeyed over the range of conditions studied here, becoming very nonlinear at cos θ < 0.5. If the linear region of the Zisman plot for cos θ > about 0.5 is evaluated as shown in Figure 10, $\gamma_{LV}{}^c$ = 25.5 mN/m and β = 0.045. For comparison, when $\gamma_{LV}{}^c$ of difluoroethene = 25 mN/m, values of β are typically between 0.03 and 0.04 (20).

In studies of wetting of single-component surfactant solutions on a hydrophobic surface (generally polymers), the Gibbs equation has been combined with the Young equation to deduce surfactant adsorption at the solid/liquid interface from contact angles and vapor/liquid surface tensions (14,36,37). Since both the subsaturated NaDS and saturated CaC$_{12}$ were present in solution in our system, the single-component analysis done in those studies cannot be applied to the data presented here to deduce surfactant adsorption at the solid/liquid interface and compared to adsorptions measured directly. In other studies on polymers, direct measurement of surfactant adsorption was generally
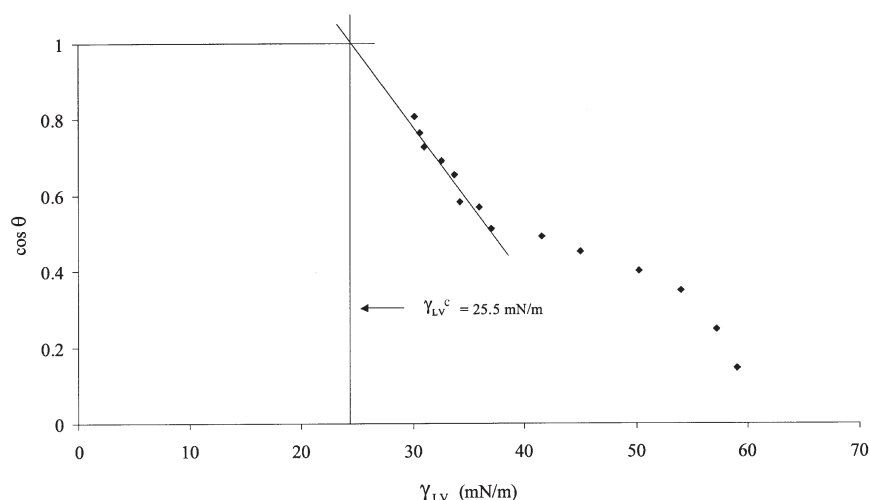
FIG. 10. Zisman plot. γ_{LV}^{c} is the critical surface tension for the CaC_{12}. For other abbreviation see Figure 1.
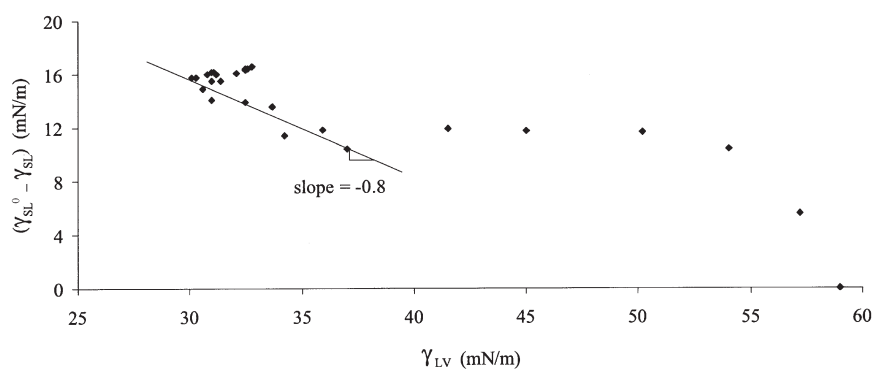
FIG. 11. Relationship between $\gamma_{SL}^{0} - \gamma_{SL}$ and γ_{LV}. For abbreviations see Figures 1 and 8.

not done for comparison with the deduced value. The general conclusion from studies of surfactant solution wetting on hydrophobic polymers is that the Zisman equation works because the reduction in γ_{SL} [or increase in $(\gamma_{SL}^{0} - \gamma_{SL})$] is approximately the same as the reduction in γ_{LV} with increasing surfactant concentration. Therefore, the γ_{LV} term in Equation 6 coincidentally reflects interfacial tension reduction at both the liquid/vapor and the solid/liquid interfaces, since they mirror each other. This is shown for our system in Figure 11, where the slope of $\gamma_{SL}^{0} - \gamma_{SL}$ vs. γ_{LV} is -0.8 for the linear region of the Zisman plot ($\gamma_{LV} < 40$ mN/m), compared to -1 if the reductions in γ are identical. As with single surfactants on hydrophobic plastics, the reduction in γ_{SL} is comparable with that in γ_{LV}, explaining why the Zisman plot works in this concentration range. The Zisman equation is empirical and is more often used in applications under conditions far beyond those originally intended. This work shows that this can be a dangerous practice for surfactant solutions.

ACKNOWLEDGMENTS

REFERENCES

1. Oner, D., and T.J. McCarthy, Ultrahydrophobic Surfaces. Effect of Topography Length Scales on Wettability, *Langmuir 16*: 7777 (2000).
2. Johnson, R.E., and R.H. Dettre, Wetting of Low-Energy Surfaces, in *Wettability*, edited by J.C. Berg, Marcel Dekker, New York, 1993, p. 1.
3. Hauthal, H.G., P. Jurges, L. Mohle, and U. Ohlerich, Synergism in the Wetting Properties of Ternary Surfactant Mixtures, *J. Surfact. Deterg. 2*:175 (1999).
4. Bahr, M.V., F. Tiberg, and B.V. Zhmud, Spreading Dynamics of Surfactant Solutions, *Langmuir 15*:7069 (1999).
5. Guy, D.W., R.J. Crawford, and D.E. Mainwaring, The Wetting Behavior of Several Organic Liquids in Water on Coal Surfaces, *Fuel 75*:238 (1996).
6. Shiao, S.Y., V. Chhabra, A. Patist, M.L. Free, P.D.T. Huibers, A. Gregory, S. Patel, and D.O. Shah, Chain Length Compatibility Effects in Mixed Surfactant Systems for Technological Applications, *Adv. Colloid Interface Sci. 74*:1 (1998).
7. Alexandrova, L., and L. Grigorov, The Three-Phase Contact Parameters of Thin Water Films on Mineral Surfaces, *Colloids Surf. 131*:265 (1998).
8. Chesters, A.K., A. Elyousfi, A.M. Cazabat, and S. Vilette, The

Influence of Surfactants on the Hydrodynamics of Surface Wetting, *J. Petrol. Sci. Eng. 20*:217 (1998).

9. Luner, P.E., S.R. Babu, and S.C. Mehta, Wettability of a Hydrophobic Drug by Surfactant Solutions, *Int. J. Pharm. 128*:29 (1996).

10. Garti, N., and H. Zour, The Effect of Surfactants on the Crystallization and Polymorphic Transformation of Glutamic Acid, *J. Cryst. Growth 172*:486 (1997).

11. Lin, C.H., N. Gabas, and J.P. Canselier, Prediction of Growth Morphology of Amino Acid Crystals in Solution I. α-Glycine, *J. Cryst. Growth 191*:803 (1998).

12. Paton, O., and F.I. Talens-Alesson, Colloidal Flocculation of Micellar Solutions of Anionic Surfactants, *J. Surfact. Deterg. 3*:399 (1998).

13. Garrett, P.R. The Mode of Action of Antifoams, in *Defoaming*, edited by P.R. Garrett, Marcel Dekker, New York, 1993, p. 1.

14. Rosen, M.S., *Surfactants and Interfacial Phenomena*, 2nd edn., John Wiley & Sons, New York, 1989, pp. 224, 240.

15. Hudson, D.M., The Use of Contact Angle Analysis to Determine Surface Cleanliness, *Met. Finish. 10*:26 (1997).

16. Kwok, D.Y., T. Gietzelt, K. Grundke, H.J. Jacobasch, and A.W. Neumann, Contact Angle Measurements and Contact Angle Interpretation: I. Contact Angle Measurements by Axisymmetric Drop Shape Analysis and a Goniometer Sessile Drop Technique, *Langmuir 13*:2880 (1997).

17. Miwa, M., A. Nakajima, A. Fujishima, K. Hashimota, and T. Watanabe, Effect of Surface Roughness on Sliding Angles of Water Droplets on Superhydrophobic Surfaces, *Langmuir 16*: 5754 (2000).

18. Subrahmanyam, T.V., C.A. Prestidge, and J. Ralston, Contact Angle and Surface Analysis Studies of Sphalerite Particles, *Miner. Eng. 9*:727 (1996).

19. Gyorvary, E., J. Peltonen, M. Linden, and J.B. Rosenholm, Reorganization of Metal Stearate LB Films Studied by AFM and Contact Angle Measurements, *Thin Solid Films 284*:368 (1996).

20. Adamson, A.W., *Physical Chemistry of Surfaces*, 5th edn., John Wiley & Sons, New York, 1990, p. 379.

21. Serre, C., P. Wynblatt, and D. Chatain, Study of a Wetting-Related Adsorption Transition in the GA–Pb System: I. Surface Energy Measurements of Ga-rich Liquid, *Surf. Sci. 415*:336 (1998).

22. Dechabumphen, N., N. Luangpirom, C. Saiwan, and J.F. Scamehorn, Contact Angle of Surfactant Solutions on Precipitated Surfactant Surfaces, *J. Surfact. Deterg. 4*:367 (2001).

23. ASTM, *Annual Book of ASTM Standards*, Vol. 15.04, ASTM International, West Conshohocken, PA, 2003, method D1331-89.

24. Lunkenheimer, K., and K.D. Wantke, Determination of the Surface Tension of Surfactant Solution Applying the Method of Lecomte DuNoüy (ring tensiometer), *Colloid Polym. Sci. 25*:354 (1981).

25. Mukerjee, P., and K.J. Mysels, *Critical Micelle Concentrations of Aqueous Surfactant Systems*, Department of Commerce, U.S. Government, Washington DC, 1970.

26. Vora, S., A. George, H. Desai, and P. Bahadun, Mixed Micelles of Some Anionic–Anionic, Cationic–Cationic, Ionic–Nonionic Surfactants in Aqueous Media, *J. Surfact. Deterg. 2*:213 (1999).

27. Drelich, J., J.D. Miller, A. Kumar, and G.M. Whitesides, Wetting Characteristics of Liquid Drops at Heterogeneous Surfaces, *Colloids Surf. A: Physicochem. Eng. Aspects 93*:1 (1994).

28. Rodriguez, C.H., C. Chintasathien, J.F. Scamehorn, C. Saiwan, and S. Chavadej, Precipitation in Solution Containing Mixtures of Synthetic Anionic Surfactant and Soap. I. Effect of Sodium Octanoate on Hardness Tolerance of Sodium Dodecyl Sulfate, *J. Surfact. Deterg. 1*:321 (1998).

29. Scamehorn, J.F., R.S. Schechter, and W.H. Wade, Adsorption of Surfactants on Mineral Oxide Surface from Aqueous Solutions. I: Isomerically Pure Anionic Surfactants, *J. Colloid Interface Sci. 85*:463 (1982).

30. Dahanayake, M., A.W. Cohen, and M.J. Rosen, Relation of Structure to Properties of Surfactant: 13. Surface and Thermodynamic Properties of Some Oxyethylenated Sulfates and Sulfonates, *J. Phys. Chem. 90*:2413 (1986).

31. Harwell, J.H., and J.F. Scamehorn, Adsorption from Mixed Surfactant Systems, in *Mixed Surfactant Systems*, edited by K. Ogino and M. Abe, Marcel Dekker, New York, 1993, p. 263.

32. Rathman, J.F., and J.F. Scamehorn, Counterion Binding on Mixed Micelles, *J. Phys. Chem. 88*:5807 (1984).

33. Hanna, H.S., and P. Somasundaran, Adsorption of Sulfonates on Reservoir Rocks, *J. Colloid Interface Sci. 19*:221 (1979).

34. Smith, S.A., B.J. Shiau, J.H. Harwell, J.F. Scamehorn, and D.A. Sabatini, Performance and Chemical Stability of a New Class of Ethoxylate Sulfate Surfactants in a Subsurface Remediation Application, *Colloids Surf. 116*:225 (1996).

35. Zisman, W.A., Contact Angle, Wettability and Adhesion, in *Advances in Chemistry Series 43*, edited by R.F. Gould, American Chemical Society, Washington DC, 1964, p. 1.

36. Gau, C.S., and G. Zografi, Relationships Between Adsorption and Wetting of Surfactant Solutions, *J. Colloid Interface Sci. 140*:1 (1990).

37. Pyter, R.A., Zografi, G., and P. Mukerjee, Wetting of Solids by Surface–Active Agents: The Effects of Unequal Adsorption to Vapor–Liquid and Solid–Liquid Interfaces, *J. Colloid Interface Sci. 89*:144 (1982).

Piyada Balasuwatthi presently works at Bangkok Synthetic Company Limited, in Thailand as a process engineer. She received her B.S. in Chemical Engineering from Srinakharinvirot University and M.S. in Petrochemical Technology from Chulalongkorn University in Bangkok.

Nimit Dechabumphen presently works at Rhodia Co., Ltd. (Thailand) as a sales executive. He received his B.S. in Chemical Technology and M.S. in Petrochemical Technology from Chulalongkorn University in Bangkok.

Chintana Saiwan is currently associate professor in petrochemical technology at the Petroleum and Petrochemical College in Chulalongkorn University in Bangkok. She received her B.S. in Chemistry at Kasetsart University and her Ph.D. in Chemistry at the University of Missouri–Columbia. Her research interests include the fundamentals and applications of surfactants.

John Scamehorn holds the Asahi Glass Chair in Chemical Engineering and is Director of the Institute for Applied Surfactant Research at the University of Oklahoma. He received his B.S. and M.S. at the University of Nebraska and his Ph.D. at the University of Texas, all in Chemical Engineering. Dr. Scamehorn has worked for Shell, Conoco, and DuPont and has been on a number of editorial boards for journals in the area of surfactants and of separation science. He has coedited four books and coauthored over 150 technical papers. His research interests include surfactant properties important in consumer product formulation and surfactant-based separation processes.